© 2015. Published by The Company of Biologists Ltd | Journal of Experimental Biology (2015) 218, 3845-3854 doi:10.1242/jeb.124834

RESEARCH ARTICLE

A simple behaviour provides accuracy and flexibility in odour plume tracking – the robotic control of sensory-motor coupling in silkmoths

Noriyasu Ando* and Ryohei Kanzaki

ABSTRACT

Odour plume tracking is an essential behaviour for animal survival. A fundamental strategy for this is to move upstream and then across-stream. Male silkmoths, *Bombyx mori*, display this strategy as a pre-programmed sequential behaviour. They walk forward (surge) in response to the female sex pheromone and perform a zigzagging 'mating dance'. Though pre-programmed, the surge direction is modulated by bilateral olfactory input and optic flow. However, the nature of the interaction between these two sensory modalities and contribution of the resultant motor command to localizing an odour source are still unknown. We evaluated the ability of the silkmoth to localize an odour source under conditions of disturbed sensory-motor coupling, using a silkmoth-driven mobile robot. The significance of the bilateral olfaction of the moth was confirmed by inverting the olfactory input to the antennae, or its motor output. Inversion of the motor output induced consecutive circling, which was inhibited by covering the visual field of the moth. This suggests that the corollary discharge from the motor command and the reafference of self-generated optic flow generate compensatory signals to guide the surge accurately. Additionally, after inverting the olfactory input, the robot successfully tracked the odour plume by using a combination of behaviours. These results indicate that accurate guidance of the reflexive surge by integrating bilateral olfactory and visual information with innate pre-programmed behaviours increases the flexibility to track an odour plume even under disturbed circumstances.

KEY WORDS: Odour-source localization, Corollary discharge, Reafference, Chemotaxis, Optomotor response, Sensory-motor integration

INTRODUCTION

Tracking an attractive odour plume and finding its source is an essential task animals must perform to find food, nests and mating partners. Odorants are often diffused and flow in a stream. Therefore, the spatiotemporal information of the odorants is ceaselessly changing in the environment (Murlis and Jones, 1981). Consequently, based on the distance from the odour source, animals do not always have access to a continuous concentration gradient of odorants. To track the odorants and localize the odour source, animals have evolved various behaviours based on a fundamental strategy that largely comprises two stereotyped behaviours. Once animals receive an odorant, they move upstream to track it (surge), and if they lose the odorant, they move across the stream (casting) or change their direction to re-contact it (Vickers, 2000; Willis, 2008). Insects are useful models for studying odour tracking as they display this fundamental strategy in both walking (Tobin, 1981; Tobin and Bell, 1986; Willis and Avondet, 2005) and flying (Kennedy and Marsh, 1974; Kennedy, 1983; Willis and Baker, 1987; Baker and Vogt, 1988; Mafra-Neto and Carde, 1994; Vickers and Baker, 1994; Budick and Dickinson, 2006; van Breugel and Dickinson, 2014).

If animals enter the odour plume and repetitively receive the odorants as they approach the odour source, or if they are in a still flow, a local gradient of odour concentration would also be an important cue for orienting themselves according to the direction of the source (chemotaxis) (Gomez-Marin et al., 2010). However, this strategy would be valid for animals during walking (Martin, 1965; Borst and Heisenberg, 1982), as opposed to flying (Vickers, 2006; van Breugel and Dickinson, 2014), because they would be moving more slowly and would have access to the local concentration gradient. There are two strategies to detect bilateral odour cues for steering: klinotaxis (the sequential sampling of a spatial gradient) and osmotropotaxis (the simultaneous sampling of a concentration gradient using spatially separated olfactory organs). Typical klinotaxis in insects is observed in *Drosophila* larvae, which move their heads laterally and use their olfactory organs (dorsal organ) to spatially sample the gradient (Gomez-Marin et al., 2011). However, adult flies have the ability to turn to the side with a higher odour concentration by using osmotropotaxis (Borst and Heisenberg, 1982; Duistermars et al., 2009; Gaudry et al., 2013).

Considering the complexity of the spatiotemporal distribution of odorants, the multiple uses of the pre-programmed behaviour and chemotaxis in different odour contexts would improve odour-tracking capability (Gaudry et al., 2012). A male silkmoth, *Bombyx mori* (Linnaeus 1758), may utilize these multiple strategies. It responds to the conspecific female sex pheromone and walks towards the female while fluttering its wings (Kramer, 1975). This 'mating dance' emerges from stereotyped sequential behaviours: straight-line walking (surge) during pheromone reception and zigzagging followed by a loop when pheromones are no longer received (Kanzaki et al., 1992). This sequence is reset and restarted with a surge once pheromones are again detected and is comparable to the aforementioned mechanisms of surge and casting of flying insects (Kramer, 1997; Kanzaki, 1998). Behavioural and neurophysiological evidence indicates that the surge is a reflex, while zigzagging and looping are pre-programmed behaviours (we therefore do not discriminate looping from zigzagging) (Olberg, 1983; Kanzaki and Mishima, 1996; Mishima and Kanzaki, 1999; Wada and Kanzaki, 2005; Kanzaki, 2007). Recent behavioural studies reported that the surge direction is modulated by the bilateral olfactory input and optic flow, and is less affected by the wind direction (Takasaki et al., 2012; Pansopha et al., 2014), suggesting

Research Center for Advanced Science and Technology, University of Tokyo, Meguro, Tokyo 153-8904, Japan.

*Author for correspondence (ando@brain.imi.i.u-tokyo.ac.jp)

Received 7 May 2015; Accepted 5 October 2015

Journal of Experimental Biology (2015) 218, 3845-3854 doi:10.1242/jeb.124834

that while the silkmoth decides the surge direction through osmotropotaxis, the course control is stabilized by the optomotor response (compensatory movements in response to optic flow). However, silkmoths do not show the optomotor response during the zigzagging phase (Pansopha et al., 2014), suggesting that zigzagging is simply controlled by internal mechanisms. This makes the surge the only chance to change direction based on external sensory information. But, these results were obtained from behavioural responses to well-controlled artificial olfactory and visual stimuli. Therefore, it is still unclear how surge control is significant for localization of an odour source, how moths integrate the bilateral olfactory input to generate a directional command, and how these multiple strategies are utilized in different contexts.

To answer these questions, we conducted a novel behavioural experiment using an insect-controlled mobile robot (Emoto et al., 2007; Ando et al., 2013). This two-wheeled robot was designed as an experimental environment in which a tethered walking insect receives sensory information from the real world. In this study, the robot was driven by a male silkmoth in the cockpit, where it acquired olfactory information through two air suction tubes, and visual information through a transparent canopy covering the cockpit. To investigate the significance of bilateral olfaction for odour source localization, we altered the odour gradient sampled by the bilateral antennae of the moth by changing the positions of the left and right air suction tubes. Additionally, we examined the influence of the visual input. The results of these experiments suggest that the corollary discharge from the odour-driven turning command and reafference of self-generated optic flow generate compensatory signals to accurately guide the surge. We also observed that the robot with an inverted bilateral olfactory input tracked the odour plume by using a combination of surge and zigzagging. Our study indicates that the accurate guidance of the surge and pre-programmed behaviours generate flexible strategies to robustly track an odour plume.

MATERIALS AND METHODS

Experimental animals

We used 2–8 day old adult male silkmoths (*B. mori*), which were reared in our laboratory or purchased as pupae. All larvae and pupae were reared at 25–27°C, and adult moths were kept at 15°C before the behavioural experiments, which were conducted at room temperature (22–28°C).

Insect-controlled robot

The specifications of the robot and animal preparations were the same as those described in previous experiments (Emoto et al., 2007; Ando et al., 2013). Specifically, the silkmoth was tethered dorsally at the tip of a bar with an adhesive (G17, Konishi, Osaka, Japan) and placed on an air-floated white polystyrene ball (50 mm in diameter; Fig. 1A). The rotation of the ball by the moth's walking behaviour was measured with an optical mouse sensor (HDNS-2000, Agilent Technologies, Santa Clara, CA, USA) with a resolution of 0.254 mm; an on-board microcontroller (ATMEGA8, Atmel, San Jose, CA, USA) calculated the turn angular velocity and forward velocity of the ball and controlled the rotation of two brushless DC motors (EC-45, Maxon Motor, Sachseln, Switzerland) at a control frequency of 1 kHz. The gain between the angular velocity and forward velocity of the silkmoth and those of the robot was set at 1.

For the present study, we attached air suction tubes and a transparent canopy to improve odour delivery to the moth. Two flexible polyethylene tubes (15 mm in diameter) were placed on the right and left sides of the robot, each connected to a fan (1606KL-04W-B50, Minebea Motor Manufacturing, Tokyo, Japan). The suctioned air was separated by a partition and provided to the antennae on each side of the on-board moth in the transparent canopy, which acted as a flow channel (Fig. 1A; Movie 1). Two white LEDs maintained constant illumination (280 lx) in the canopy even when the visual field was covered (see below). The wind speed in the canopy was 0.5 m s^{-1}, which is comparable to the air speed generated by wing fanning in untethered male silkmoths (0.3–0.4 m s^{-1}; Loudon and Koehl, 2000) and was not affected by the heading of the robot in the wind tunnel. The surge direction of silkmoths is less affected by wind direction (Takasaki et al., 2012); therefore, the constant air flow in the canopy would not greatly modulate the surge direction.

For manipulation of the sensory-motor relationship, we simply crossed the air suction tubes to invert the olfactory input, and the control cables of the motors to invert the motor output. For covering the visual field of an on-board moth, we attached white paper to the canopy of the robot. The paper covered 105 deg and 90 deg of the horizontal and vertical visual fields of the moth, respectively. These manipulations were further combined with varying sizes of the gap between the two tubes (wide gap, 90 mm; narrow gap, 20 mm) to alter the slope of the odour gradient acquired by the antennae of the on-board moth. The actual gap between the two antennae of male silkmoths was ca. 2.5 mm at the proximal ends and 15 mm at the distal ends; therefore, the narrow gap was comparable to the actual antennal gap of silkmoths, whereas the wide gap was larger than the actual antennal gap. Using a smoke test, we confirmed that varying the size of the tube gap effectively altered the odour sampling area (Fig. S1).

Olfactory stimulation and odour plume tracking test

We used an odour delivery system as previously described (Takasaki et al., 2012; Pansopha et al., 2014). To analyse the relationship between the stimulus side and the walking direction at behavioural onset, we applied a single puff of synthetic bombykol stimulus [(*E*,*Z*)-10,12-hexadecadien-1-ol; a principal component of the female pheromone] to one of the air suction tubes. To do this, we applied 2000 ng of bombykol dissolved in *n*-hexane to a piece of filter paper, put this into a glass pipette, inserted the pipette into the suction tube and released air flow (1 l min^{-1}) over 500 ms.

For the odour plume tracking test, we released 200 ng of bombykol at 2 Hz (200 ms of bombykol puffing alternating with 300 ms pauses) in a wind tunnel (1800×900×300 mm L×W×H; wind speed, 0.7 m s^{-1}). We estimated the boundaries of the odour plume in the wind tunnel by using $TiCl_4$ smoke (Fig. 1B). We also estimated the odour concentration in the wind tunnel and in the canopy of the robot using 80% ethanol and a hot-wire semiconductor sensor (CH-ETiXP, New Cosmos Electronic, Osaka, Japan). We confirmed that the odour suction system could deliver a fine temporal structure of odour concentration from the odour plume (Fig. S2). The start position of the robot was 600 mm downwind from an odour source with a heading angle relative to the odour source (θ) of 0 deg (i.e. towards the odour source; Fig. 1B). Successful localization was judged as follows: either (1) the position of an on-board moth enters a goal area (120 mm in radius from the centre of the odour source) with $|\theta| \leq 45$, or (2) the tip of a tube contacts the odour source (the tip is located within 20 mm from the centre of the odour source). Trials in which the robot did not localize the odour source within 240 s, ceased moving, or hit a wall outside the odour plume were regarded as failures. We used 196 moths for this study, and each moth was used only once for each test (a single-puffed stimulus for each side and an odour plume tracking test), except for seven moths which were used twice for different experimental conditions on different days.

Data analysis

All tracking behaviours of the robot were captured by video camera (HDR-XR520V, Sony, Tokyo, Japan) at 30 frames s^{-1}, and the position and body angle of the robot on each frame were acquired using a custom-built Java program. These time-series data were smoothed with a Gaussian window (bandwidth 0.5 s). All analyses were conducted using R (R Development Core Team, 2010). The significance level of all statistical tests was set at $P<0.05$.

The success rate (%) in each experimental condition was calculated as follows:

$$\text{Success rate} = 100 \times \frac{N_{\text{success}}}{N}, \quad (1)$$

Journal of Experimental Biology (2015) 218, 3845-3854 doi:10.1242/jeb.124834

where N is the total number of trials and $N_{success}$ is the number of trials in which the robot localized the odour source. To evaluate the overall performance for localization of the odour source, we compared the time course of the success rate (success rate curve), which represents both the success rate and the time taken for localization. We used a Kaplan–Meier survival analysis (Therneau, 2014) and defined 'survival' as follows:

$$\text{Survival} = 1 - \frac{N_{success}}{N}. \quad (2)$$

Differences between the Kaplan–Meier curves of survival were tested using a log-rank test. Finally, the Holm–Bonferroni method (Holm, 1979) was used to adjust the P-value (adjusted P) for multiple comparisons.

Though it is difficult to precisely discriminate the surge or zigzagging phases (Fig. 1C) from a tracking trajectory, we segmented each trajectory into two phases, termed run and turn (Fig. S3). The run phase mainly included surges and was defined as any straight-line movement (at a turn angular velocity ≤5 deg s^{-1}) of the robot lasting longer than 0.5 s, at a forward velocity >5 mm s^{-1}, with a travel distance >5 mm. The turn phase was defined as the turning of the robot in a given direction lasting longer than 0.5 s, with an angular velocity >5 deg s^{-1}, when the total angle turned was >30 deg (Ando et al., 2013). This would include both curved surging in response to a bilateral difference in the olfactory input and zigzagging in response to previous behavioural observations (Kanzaki et al., 1992; Pansopha et al., 2014). Behaviours that did not correspond to these criteria were regarded as null periods that included stopping and switching direction, which were not accounted for in our analyses. Consecutive runs or turns in the same direction with a null period within 0.5 s were regarded as the same event. As an index of circling, we calculated the mean turn angle as

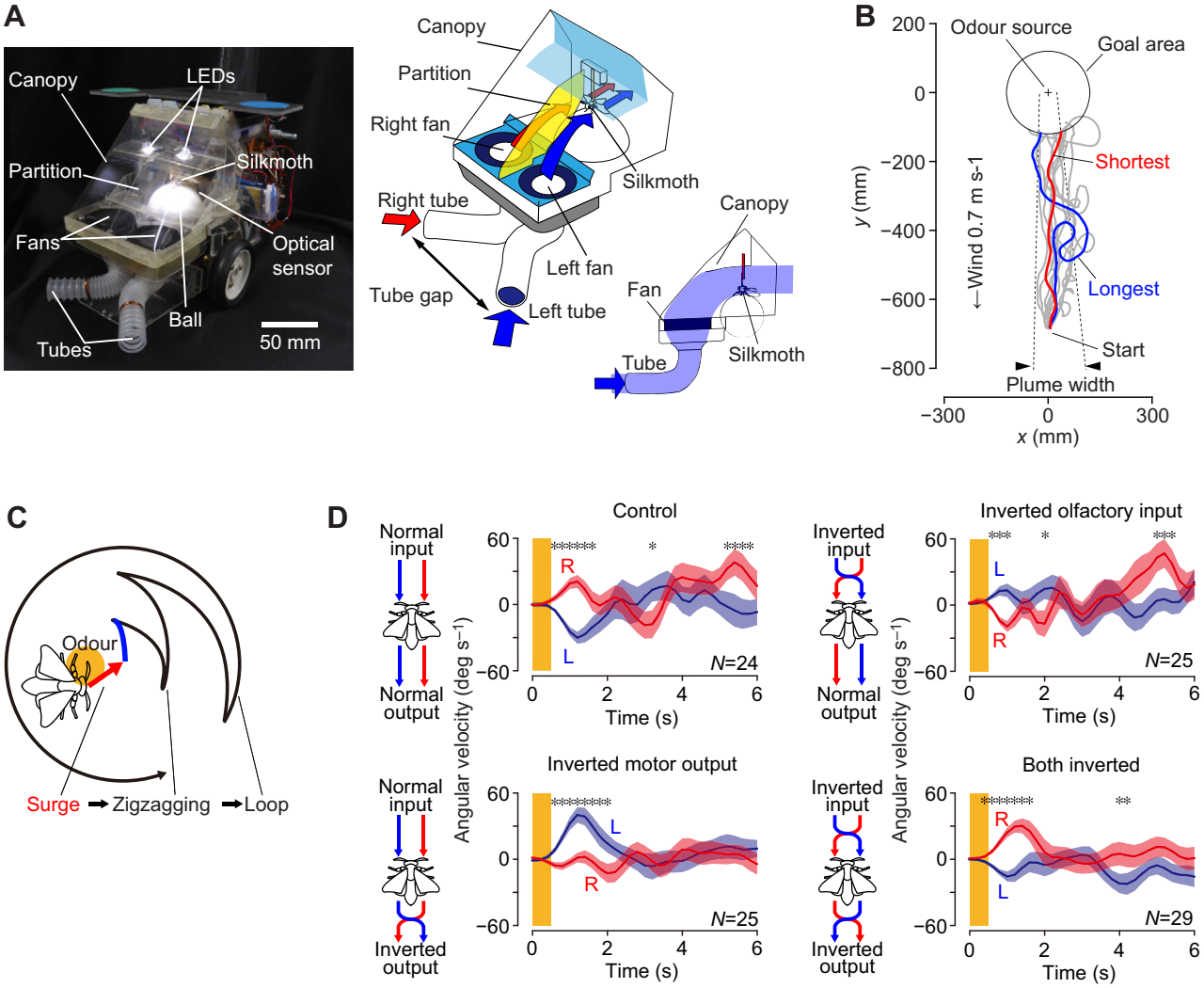

Fig. 1. Manipulation of the sensory-motor relationship of the robot. (A) An insect-controlled mobile robot and schematic drawings of the odour suction system. Air flow on each side is indicated by red or blue arrows, or by the blue shaded area in the side view (right). (B) Sample trajectories of the robot with a tube gap of 90 mm (N=12; the trajectories with the tube tip positions are shown as the control condition in Fig. S5A). The trials with the shortest (25.0 s) or the longest (60.3 s) time taken for localization are indicated as red and blue lines, respectively (median: 35.1 s). The other trials are coloured grey. The position of the odour source and the estimated boundaries of the odour plume are indicated as a plus sign and dashed lines, respectively. A circle indicates the goal area for judging success in localization (see Materials and methods). (C) Schematic drawing of the pheromone-triggered programmed behaviour of a male silkmoth. The direction of the surge (red arrow) and of the first turn during zigzagging (blue line) is towards the side with the higher odour concentration (orange). Note that the actual behaviour during zigzagging and looping consists of point turns. (D) Time course of the robot's angular velocity after a single puffed bombykol stimulus applied to one of the air suction tubes. The four panels indicate control (normal olfactory input and normal motor output), inverted olfactory input, inverted motor output, and both inverted (inverted olfactory input and inverted motor output) conditions. The red and blue lines indicate the mean angular velocity after the odour stimulus was applied to the right (R) or left side (L), respectively, averaged every 200 ms. The red and blue shaded areas indicate the standard error. The positive and negative angular velocities indicate clockwise and anticlockwise directions, respectively. The orange shaded area indicates an odour stimulus of 2000 ng bombykol that was released over 500 ms. An asterisk indicates a significant difference in angular velocity between the stimulus sides at each 200 ms time bin (paired t-test, *P<0.05).

Journal of Experimental Biology

Journal of Experimental Biology (2015) 218, 3845-3854 doi:10.1242/jeb.124834

follows:

$$\text{Mean turn angle} = \frac{1}{n_{\text{turn}}}\sum|\alpha_{\text{turn}}|, \quad (3)$$

where n_{turn} indicates the number of turn phases and α_{turn} indicates the turn angle during each turn phase.

To analyse the tendency to perform alternating short turns towards the odour source, we fitted a linear mixed-effects model (Pinheiro et al., 2013) to the relationship between the onset of heading (θ_{onset}) and turn angle (α) during the corresponding phases. We focused on surges or short turns during zigzagging ($|\alpha|\leq180$ deg; the range covered the turn angle in the first turn during zigzagging; Kanzaki et al., 1992; Pansopha et al., 2014), which was initiated when the robot headed towards the odour source ($|\theta_{\text{onset}}|\leq90$ deg). Considering the variances within individuals as random effects, we used a random slopes and intercepts model. The significance of the slope of a fixed effect was tested at a significance level of $P<0.05$. The total number of behavioural segments and those corresponding to the criteria of the surge or short turn are shown in Table S1.

We used a paired *t*-test to compare the angular velocity between stimulus sides and Steel's test to compare parameters in the manipulated and control conditions.

RESULTS

The insect-controlled mobile robot provides arbitrary odour conditions to a moth

The silkmoth was tethered dorsally and placed on an air-floated polystyrene ball in the robot. Once the moth received the pheromone, it performed odour-tracking behaviour and controlled the robot. To test the localization of the odour source, the robot was placed in the odour plume, 600 mm downwind of the wind tunnel (wind speed: 0.7 m s^{-1}). We observed that the robot tracked the odour inside the plume and localized the odour source in all 12 trials (Fig. 1B), which was comparable to the odour-tracking behaviour of the walking silkmoth tested under the same odour conditions (Fig. S4).

The directions of the surge and the first turn during zigzagging are determined by a difference in odour concentration at the two antennae (Fig. 1C; Kanzaki et al., 1992; Takasaki et al., 2012). Therefore, we applied two types of manipulation to the robot to investigate the significance of the bilateral olfactory input. In the first, the position of the tubes was inverted (inverted olfactory input condition); in the second, the motor control on the right and left sides was inverted (inverted motor output condition). These manipulations were expected to switch the robot's response to a higher odour concentration from attraction to avoidance. To test the behavioural effect of the manipulations, we applied a single puff of bombykol stimulus into the tube on the right or left side. Within 1–2 s of stimulus application (corresponding to the surge and the first turn during zigzagging; Fig. 1D), the angular velocity towards the ipsilateral side of the stimulus was significantly larger than that elicited by the contralateral side of the stimulus in the control (normal olfactory input and normal motor output; paired *t*-test, $P<0.05$), suggesting that the robot showed positive chemotaxis. Inverting the olfactory input or motor output reversed the turning behaviour, and inverting both olfactory and motor outputs restored the turning behaviour to normal (Fig. 1D). These results indicated that we could easily and non-invasively manipulate the robot's chemotactic response to positive or negative odour concentration gradients by inverting the olfactory input and/or the motor output.

Accurate bilateral olfactory input is helpful for efficient odour source localization

All tests for odour source localization were conducted in the wind tunnel (wind speed: 0.7 m s^{-1}; Fig. 1B; Fig. S2), where bombykol was released at 2 Hz to elicit consecutive surges in the odour plume (Kanzaki et al., 1992; Pansopha et al., 2014). In addition to the aforementioned manipulations of the sensory-motor relationship, we altered the size of the gap between the two tubes [a wide gap (90 mm) and a narrow gap (20 mm)] to alter the difference in the odour concentration sampled between bilateral antennae (Fig. 2A).

As shown in Fig. 1B, under the control condition (normal sensory-motor relationship) with the wide gap, the robot continuously headed towards the odour source and showed straight trajectories in the odour plume, indicating that the on-board moth frequently performed consecutive surges in the plume (Fig. S5A, Movie 2). The robot localized the odour source in all 12 trials and the success rate (the percentage of trials in which the robot localized the odour source) reached 100%. However, trials with the inverted olfactory input or inverted motor output showed complicated trajectories (Fig. S5A, Movie 2) and a lower success rate (inverted olfactory input, 61.5%; inverted motor output, 58.3%). To evaluate the overall performance for localization of the odour source among the four sensory-motor conditions, we compared the time course of the success rate (success rate curve). The success-rate curve of the inverted olfactory input or inverted motor output conditions was far below that of the control (Fig. 2Bi) and there were significant differences between them (inverted olfactory input, adjusted $P<0.01$; inverted motor output, adjusted $P<0.001$; log-rank test of survival curves with the Holm–Bonferroni method for multiple comparisons; Fig. 2Bi), i.e. there was a lower success rate and/or a longer time for localization in these manipulated conditions. These results indicate that directional control of the surge by the bilateral olfactory input is necessary for efficient odour source localization.

Contrary to the expectation from the steering response to the one-sided olfactory stimuli (Fig. 1D), the impairment of performance for odour source localization caused by inverting either the olfactory input or the motor output was not fully restored by inversion of both the olfactory input and motor output: the success rate was 73.3% and the success rate curve was significantly lower than the control curve (adjusted $P<0.05$; Fig. 2Bi), whereas it was consistently above the curves of the inverted olfactory input or motor output.

Inversion of the olfactory input and inversion of the motor output differentially affect odour-tracking behaviour

We next narrowed the gap between the two tubes (20 mm) to reduce the difference in the odour concentration sampled by the two antennae of the moth, and tested the odour-tracking behaviour in each of the four sensory-motor relationships (Fig. S5B, Movie 3). Under control conditions, the robot exhibited a success rate of 100%, whereas inversion of either the olfactory input or motor output reduced the success rate to 75.0% and 61.5%, respectively, similar to the results with the wide gap. The success rate curves of these two manipulated conditions shifted below the control curve (Fig. 2Bii), and there were significant differences between them (inverted olfactory input, adjusted $P<0.05$; inverted motor output, adjusted $P<0.001$). In contrast to the findings with the wide tube gap, however, the success rate curve of the inverted motor output with the narrow gap was consistently below the curve of the inverted olfactory input. Furthermore, although the inversion of both the olfactory input and motor output restored the success rate (78.6%) and the success rate curve was consistently above that of the inverted motor output, the curve was still comparable to that of the inverted olfactory input and consistently below the control condition (adjusted $P<0.05$; Fig. 2Bii). These results indicate that with the narrow tube gap, which reduced the slope of the

Journal of Experimental Biology (2015) 218, 3845-3854 doi:10.1242/jeb.124834

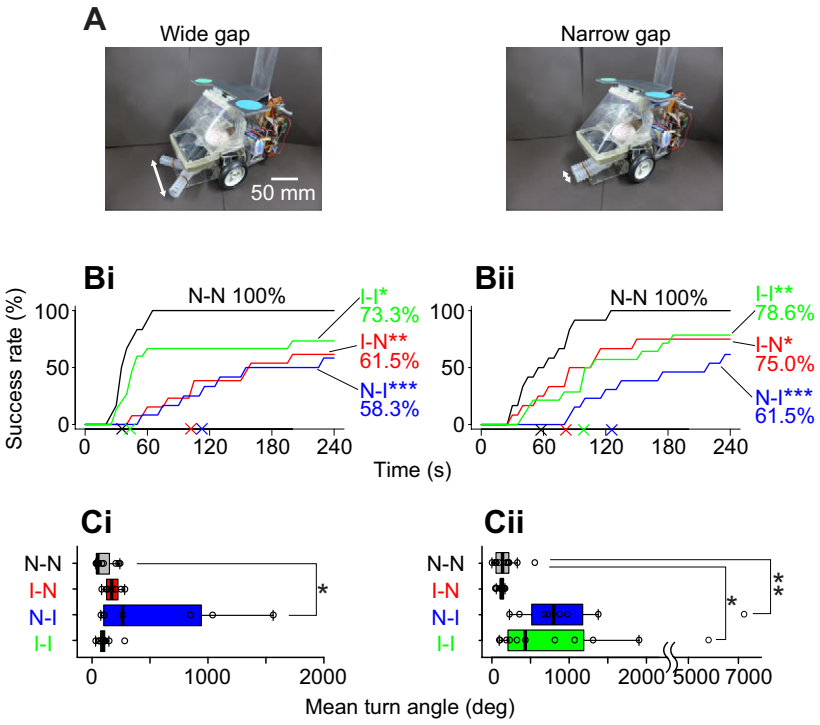

Fig. 2. Odour-tracking performance in different sensory-motor conditions. (A) The wide (90 mm) and narrow (20 mm) tube gap (arrows) conditions. (B) Time course of the accumulated success rate with the wide gap (i) and narrow gap (ii) plotted every 5 s. The final success rate is given beside each curve. Asterisks indicate a significant difference from the control (N-N) condition in the same panel, according to the log-rank survival test (see Materials and methods) followed by the Holm–Bonferroni method for multiple comparisons (*P<0.05, **P<0.01, ***P<0.001; P-values were adjusted). The crosses on the x-axis indicate the median time taken for localization in each condition. N-N (black), normal olfactory input and normal motor output (control; N=12 wide, N=12 narrow); I-N (red), inverted olfactory input and normal motor output (N=13 wide, N=12 narrow); N-I (blue), normal olfactory input and inverted motor output (N=12 wide, N=13 narrow); I-I (green), inverted olfactory input and inverted motor output (N=15 wide, N=14 narrow). All trajectories are shown in Fig. S5. (C) Mean turn angle of the successful trials with the wide gap (i) and narrow gap (ii). The mean turn angle was calculated as the sum of the turn angle divided by the number of turns. Individual data are summarised in a boxplot. The left and right sides of a box indicate the first and third quartiles, and the bar represents the median. The whiskers indicate 1.5× interquartile range. Asterisks indicate a significant difference from the control data, according to Steel's test (*P<0.05, **P<0.01).

concentration gradient sampled by the bilateral antennae, the ability to localize the odour source was strongly impaired by the inversion of the motor output as compared with the inversion of the olfactory input.

The difference between the inverted olfactory input and inverted motor output was also apparent in the tracking trajectories with both wide and narrow tube gaps: the trajectories in the inverted motor output condition tended towards continuous circling (Fig. S5, Movies 2, 3). As an index of the continuous circling, we extracted the 'turn phase' from trajectories based on the empirical thresholds of kinematical parameters (see Materials and methods; Fig. S5) (Ando et al., 2013) and calculated the mean turn angle during a single turn phase. In this index, a large value indicates continuous circling in the same direction. The mean turn angle in the inverted motor output condition was significantly larger than that in the control condition (wide gap, P<0.05; narrow gap, P<0.01; Steel's test; Fig. 2C), whereas there were no significant differences in the mean turn angle in the inverted olfactory input condition with either wide or narrow tube gaps (P>0.05). The mean turn angle under the inversion of both the olfactory input and motor output was significantly larger than the control (P<0.05) with the narrow gap, whereas no significant difference was found with the wide gap.

Visual information is used as a reafferent signal to accurately guide the surge

Why were the behavioural consequences of inverting the olfactory input and the motor output different even though both manipulations altered the preference from a higher to a lower odour concentration? We hypothesized that the difference was due to a mismatch between the prediction and consequence of motor output: the moth compares the motor command as a corollary discharge to the behavioural consequences using a reafference of sensory signals (Sperry, 1950; von Holst and Mittelstaedt, 1950; Webb, 2004; Crapse and Sommer, 2008). In a previous study we reported that silkmoths use optic flow and perform an optomotor response only during the surge (Ando et al., 2013; Pansopha et al., 2014); therefore, we conducted further orientation tests by covering the visual field of the on-board moth (Fig. 3A).

Covering the visual field did not influence the turning preference towards the higher odour concentration side and this preference was also switched by the air suction tube manipulations (Fig. S6A). However, covering the visual field and using a wide tube gap reduced the tendency to circle in the inverted motor output condition, and there was no significant difference between the mean turn angle in the inverted motor output and control conditions (P>0.1; Fig. 3Ci; all trajectories are shown in Fig. S6B). Furthermore, inverting both the olfactory input and motor output while also covering the visual field in the wide gap condition fully restored the ability to localize the odour source, compared with the control condition, which was reflected in the 100% success rate (Fig. 3Bi). Additionally, this success rate curve was comparable to the control curve (adjusted P>0.05), whereas the curves of the inverted olfactory input or inverted motor output were significantly below the control curve (inverted olfactory input, adjusted P<0.001; inverted motor output, adjusted P<0.05). These results indicate that the continuous circling observed in the inverted motor output without covering the visual field was induced by visual information, presumably by the optic flow. Inversion of the motor output would induce an optomotor response to the similarly inverted self-generated optic flow as reported in historical studies of sensory-motor coupling (Sperry, 1950; von Holst and Mittelstaedt, 1950). This suggests the possibility that silkmoths use a corollary discharge signal, a copy of a motor command related to the surge direction, and reafference of the self-induced optic flow input to guide the surge direction accurately.

In contrast, with a narrow tube gap, after covering the visual field, the robot in the inverted motor output condition still circled continuously and the mean turn angle was significantly larger than the angle in the control condition (P<0.05; Fig. 3Cii). Furthermore, the ability to track the odour plume was not restored by inverting both the olfactory input and motor output, which was apparent from the low success rate (66.7%; Fig. 3Bii), and its success rate curve

Journal of Experimental Biology (2015) 218, 3845-3854 doi:10.1242/jeb.124834

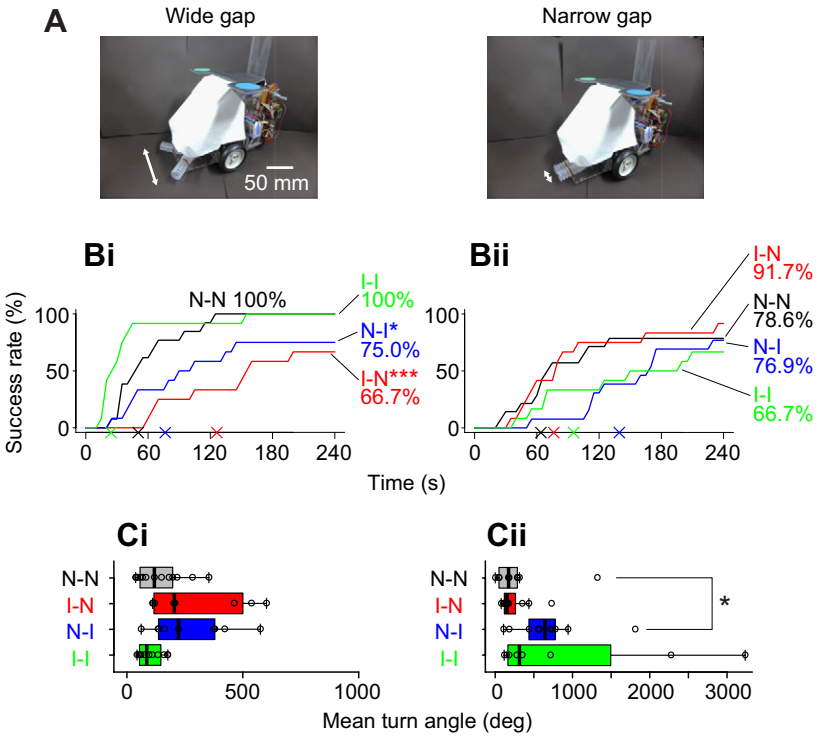

Fig. 3. Odour-tracking performance of the robot with the visual field covered. (A) The covered condition with wide (90 mm) and narrow (20 mm) tube gaps (arrows). (B) Time course of the accumulated success rate with the wide gap (i) and narrow gap (ii). N-N (black), *N*=13 wide, *N*=14 narrow; I-N (red), *N*=12 wide, *N*=12 narrow; N-I (blue), *N*=12 wide, *N*=13 narrow; I-I (green), *N*=12 wide, *N*=12 narrow. Definitions as in Fig. 2 (**P*<0.05, ****P*<0.001). All trajectories are shown in Fig. S6B,C. (C) Mean turn angle of the successful trials with a wide gap (i) and narrow gap (ii). **P*<0.05, Steel's test.

was consistently below the curves of the control and inverted olfactory input conditions. Although there were no significant differences in the success rate curves between the control and manipulated conditions (adjusted $P>0.1$), presumably due to the low performance in the control trials (success rate, 78.6%; Fig. 3Bii), these results indicate that the inversion of the motor output strongly impaired the odour source localization performance, irrespective of the inversion of the olfactory input. This suggests that, in addition to optic flow, other sensory signals might be used as reafferent signals. Indeed, the influence of the non-visual reafferent signals on motor control was particularly apparent when the moth received a lower gradient of odour concentration by the narrow gap.

Multiple strategies to track an odour plume

Odour source localization performance was impaired by inversion of the olfactory input or motor output. However, the fact that the robot localized the source in 58.3–91.7% of the manipulated trials indicated that an accurate bilateral olfactory input is not necessary for successful orientation, although it definitely improved performance. Therefore, we analysed the robot trajectories to explore strategies for tracking an odour plume.

The representative behaviour of the robot in the control condition was to move straight towards the odour source with short turns (Fig. 4A; Movie 4). Considering the tube tip positions in relation to the odour plume, the moth would use bilateral olfactory input and turn towards the higher concentration side during each turn. To characterize this behaviour, we divided a trajectory into behavioural segments (run and turn phases; Fig. S3), and calculated the heading of the robot in relation to the odour source at the onset of each behavioural segment (θ_{onset}) as well as the turn angle during a corresponding segment (α; Fig. 4B). Further, a difference in the bilateral olfactory input influences the directions of the surge and successive first short turn of zigzagging. Therefore, we focused on the corresponding behavioural segments ($|\alpha|\leq180$ deg) that were initiated at the onset of heading towards the odour source ($|\theta_{onset}|\leq90$ deg (with 0 deg being the direction of the odour source; the number of segments selected by these criteria is shown in Table S1). We then analysed the relationship between these two parameters using a linear mixed-effects model. We found significant negative slopes of a fixed effect in the control and inversion of both the olfactory input and motor output conditions when paired with a wide tube gap (control slope −0.729, $P<0.001$; slope in the double-inverted condition −0.873, $P<0.001$; Fig. 4C), indicating that the robot tended to turn towards the direction of the odour source during each behavioural segment. In these two conditions, the robot turned in the direction of the higher concentration side (Fig. 1D), and the wide gap led to the tendency that one of the tubes was inside the plume and the other was outside it while orienting (Fig. S7A). Therefore, these negative slopes were mainly due to steering based on the difference in the odour concentration between the bilateral tubes. Further, the same relationship was observed in the trials in which the visual field was covered and in which the silkmoths walked in the wind tunnel (Fig. S8).

However, the directional control by the odour gradient was not the only mechanism behind the relationship between θ_{onset} and α, because trials with a narrow gap also showed a significant negative slope even when the olfactory input alone was inverted, as well as in the control and double-inverted conditions (control slope −0.745, $P<0.001$; inverted olfactory input slope −0.438, $P<0.01$; slope in the double-inverted condition −0.374, $P<0.01$; Fig. 4D). Pre-programmed zigzagging could be another mechanism (Kanzaki, 2007) as this particularly occurs at the boundary where walking insects lose the odour plume (Willis and Avondet, 2005; Takasaki et al., 2012). Fig. 4E shows a sample trajectory from the control condition with a narrow gap, in which the robot lost the odour plume (i.e. the tube positions were out of the plume) and then turned towards it (Movie 4). In the inverted olfactory input condition, a surge from inside the plume would be directed outside of the plume because of the manipulated negative chemotaxis. If the robot successfully returns to the odour plume by turns triggered by zigzagging, it then surges outside the plume again. Fig. 4G (Movie 4) shows a trajectory from the inverted olfactory input

Journal of Experimental Biology (2015) 218, 3845-3854 doi:10.1242/jeb.124834

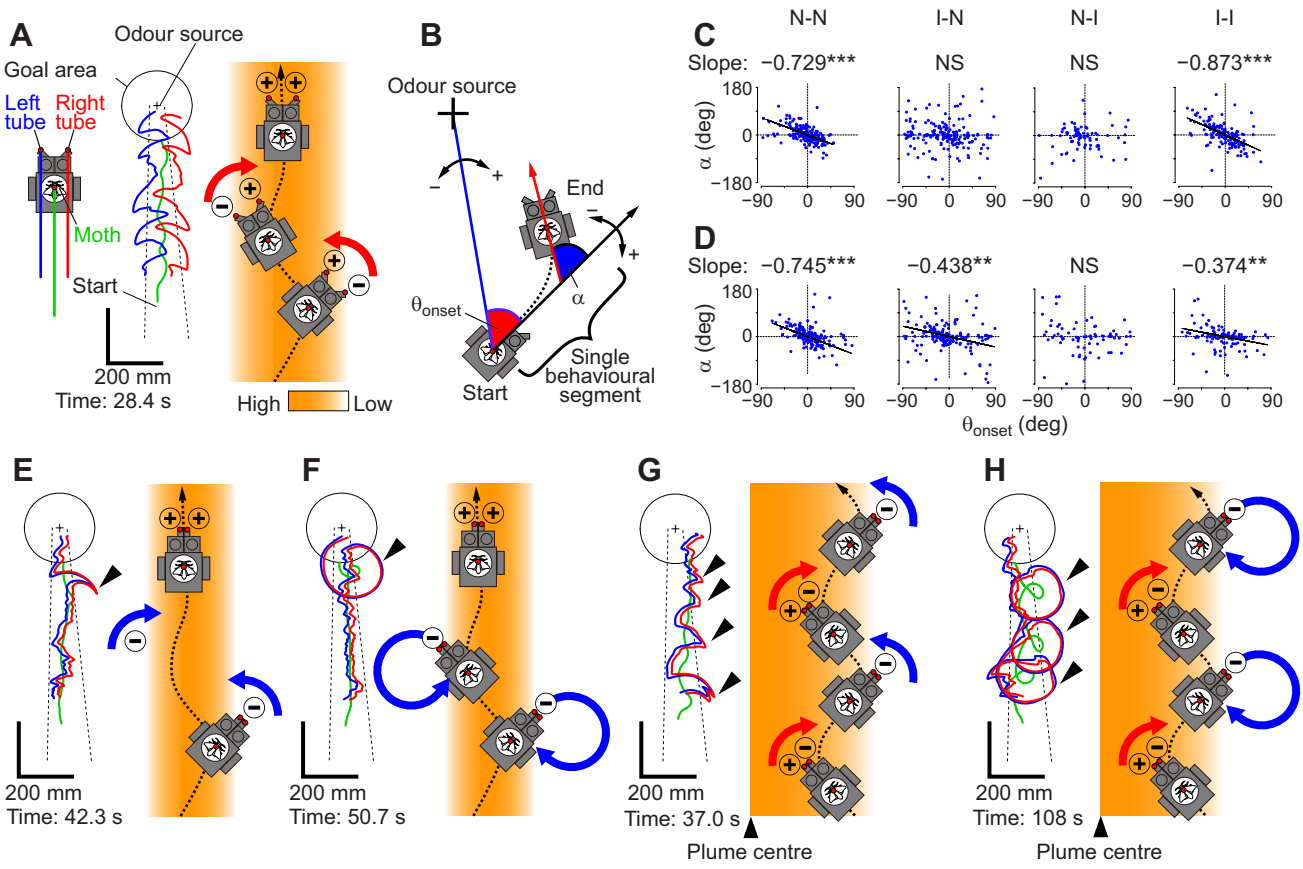

Fig. 4. Behavioural strategy to reorient towards the odour plume. (A) Tracking the odour plume using bilateral olfaction. The trajectory of a moth (green) and the tube tips on the right (red) and left (blue) in the control condition (normal input) with a wide tube gap is plotted. The time taken for localization is indicated below the plot. The schematic drawing (right) shows that the robot turns in the direction of the higher odour concentration (red arrows) by comparing the bilateral olfactory input (plus and minus signs in a schema denote the higher and lower concentration sides, respectively). (B) Definition of the turning parameters. θ_{onset} is the onset of heading towards the source (blue line) at the onset of a behavioural segment (run or turn). The turn angle (α) is the angle between the body axes of the robot before and after the behavioural segment. The clockwise and anticlockwise directions are positive and negative values, respectively. (C,D) Relationship between the onset of heading (θ_{onset}, $|\theta_{onset}| \leq 90$ deg) and turn angle (α, $|\alpha| \leq 180$ deg), as analysed by a linear mixed-effects model. The results from each condition paired with wide (C) and narrow (D) gaps are shown. Definitions as in Fig. 2. The variance between individuals was regarded as a random effect. Each of the blue points indicates a single behavioural segment (both run and turn phases were included). Each regression line indicates a fixed effect model in which a slope was statistically significant (not equal to 0; $^{**}P<0.01$, $^{***}P<0.001$; NS, non-significant, $P>0.05$). (E,F) Tracking the odour source using the pre-programmed zigzagging behaviour. Two representative trajectories in the control condition (normal input) with a narrow tube gap are displayed. The arrowheads in the trajectories indicate reorientation towards the odour plume, possibly using the pre-programmed zigzagging behaviours of small turns (E) and circles (F). Minus signs in the schemas denote failure to contact the odour plume, which triggers the zigzagging behaviour (blue arrows). (G,H) Tracking the boundary of the odour plume using imposed negative chemotaxis (red arrows) and zigzagging (blue arrows). Two representative trajectories in the inverted olfactory input condition with a narrow tube gap are displayed. The arrowheads in the trajectories indicate reorientation towards the odour plume, possibly using the pre-programmed zigzagging behaviours of small turns (G) and circles (H).

condition with a narrow gap, in which the robot tracked the odour plume with repetitive short turns, and the tube tips scanned the plume boundary. In the trials with a narrow gap, the occurrence in which only one tip was inside the plume was significantly lower than those in which both the tube tips were either inside or outside the plume (Fig. S7B), suggesting that even if the tubes with a narrow gap did not provide a concentration gradient sufficient to direct the robot towards the odour plume, the successive zigzagging turns would help it to turn back into the plume.

Larger zigzagging turns including loops at the plume boundary would also contribute towards reorienting to the odour source in both normal and disturbed sensory-motor conditions (Fig. 4F,H; Movie 4), although these would not account for the linear mixed-effects models (Fig. 4C,D). Taken together, the pre-programmed zigzagging would explain why the robot with the inverted sensory-motor relationships localized the odour source in more than 58.3% of the trials, irrespective of the complicated trajectories including continuous circling (see trajectories indicated in light blue, i.e. longer time taken for localization, ca. >60 s, in Figs S5 and S6). These observations indicate that although bilateral olfactory input is important for the efficient tracking of an odour plume, the simple sequential behaviour of silkmoths is enough to explain the various tracking trajectories even in the context of a disturbed sensory-motor relationship.

DISCUSSION

We have demonstrated that the surge direction involves the integration of the bilateral olfactory input and the self-induced visual stimuli as well as the corollary discharge of the motor command. We also show that silkmoths utilize two strategies to track an odour plume: osmotropotaxis using the bilateral olfactory input, and self-generated zigzagging. In the following discussion, we consider these two points and the significance of the robot used in this study on the insect sensory-motor system.

Journal of Experimental Biology (2015) 218, 3845-3854 doi:10.1242/jeb.124834

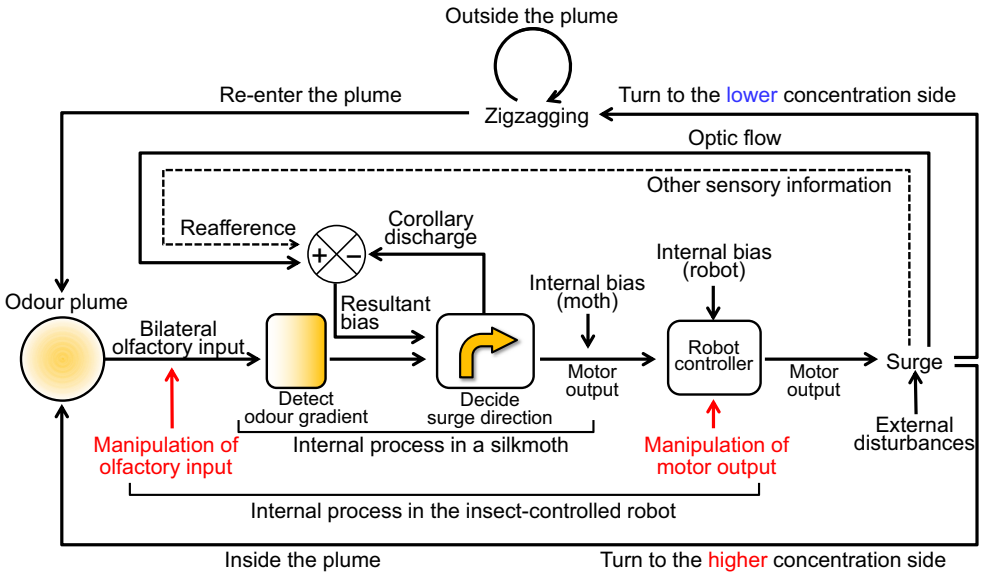

Fig. 5. Schematic drawing of a sensory-motor pathway to control surge direction and track the odour plume. When a silkmoth enters the odour plume, it acquires bilateral olfactory information to detect the odour gradient (square with colour gradient) and decides the surge direction (curved arrow). The motor output (behaviour) of the moth is then transmitted to the robot controller. During odour tracking, the corollary discharge of the motor command comprising surge direction cancels the reafference of the self-induced optic flow and other putative sensory information (dashed arrow), and the resultant bias is added to the motor command for course correction. The crossed circle indicates addition, and the plus and minus signs indicate the polarity of the signals. If the robot turns to the lower concentration side because of inversion of the olfactory input or motor output, it performs zigzagging behaviours including loops until it re-enters the plume. The inversion of the motor output inverts the polarity of the reafference. Therefore, both corollary discharge and reafference are summed and the resultant bias strengthens the intensity of turning.

Sensory motor control during surge

The information flow of the sensory-motor system in the robot with an on-board silkmoth is summarized in Fig. 5. The difference in the behavioural consequences between the inverted olfactory input and inverted motor output conditions supports the existence of reafference and corollary discharge pathways in the silkmoth. Inversion of the olfactory input simply switches the attraction to the higher odour concentration to avoidance. However, inversion of the motor output also inverts the polarity of the reafference by self-generated movements. Therefore, the inverted reafference is not cancelled by the corollary discharge, but is summed instead. The resultant bias facilitates turning in the direction that is determined by the odour gradient during the surge. Therefore, the robot strongly turns towards the lower odour concentration after inversion of the motor output, or towards the higher odour concentration after inversion of both the olfactory input and motor output. In flying insects, optic flow is used to stabilize flight direction in relation to wind direction (optomotor anemotaxis) (Kennedy and Marsh, 1974; Kennedy, 1983; Mafra-Neto and Carde, 1994; Kaissling, 1997; Chow and Frye, 2008; van Breugel and Dickinson, 2014). In walking silkmoths, the surge is a chance to actively change direction, and a bilateral olfactory input is used to decide the surge direction, rather than the wind direction (Takasaki et al., 2012). Consequently, this improves the odour source localization performance. Therefore, silkmoths would use corollary discharge to cancel the self-induced reafference to guide the surge direction accurately according to their own decision. A recent study reported the possible neural pathways involved in the corollary discharge, in which visual responses of the neurons innervating the optic lobe and the central complex in the silkmoth brain are suppressed by exposure to bombykol (Namiki et al., 2014).

In the robot with a narrow tube gap, the strong impact of inverting the motor output rather than olfactory input (Fig. 2Bii,Cii) also supports the idea of the sensory-motor control involving corollary discharge and reafferent sensory input. However, why then would inversion of both the olfactory input and motor output paired with covering of the visual field (Fig. 3Bii,Cii) not restore the ability to track an odour plume? We hypothesized that the inputs of multiple senses led to a reafferent signal, and vision might be much more important for surge control as compared with other sensory inputs such as the mechanosensory information sensing body movement (Sane et al., 2007; Dickerson et al., 2014). The wide tube gap would provide a large gradient, which is possibly a dominant factor for turning during surge as compared with the effect of the reduction in the reafference induced by covering the visual field. In contrast, as the narrow tube gap provides less spatial information of the odour gradient (Fig. S7), the surge direction would become straight. Therefore, the robot would turn in the initial direction as a result of factors that are not related to olfactory information, such as internal bias in the moth and the robot, or because of external disturbances (Fig. 5). Inversion of the motor output would strengthen this ‘unintentional’ turning, and with a narrow tube gap, it could not be compensated for by additional inversion of the olfactory input. Thus, a straight-line surge in response to the reduced difference between the bilateral olfactory input may be susceptible to non-olfactory factors and would require the guidance of other sensory inputs and accurate sensory-motor coupling.

The simple sequential behaviour generates multiple tracking strategies

Our study demonstrated that sequential behaviours in silkmoths, consisting of both the chemotactic surge and pre-programmed zigzagging behaviour, are sufficient to explain the tracking trajectories even in the absence of an accurate bilateral olfactory input (Fig. 4E–H). The use of multiple strategies such as switching between serial and bilateral odour sampling by different antennal positions or odour contexts has been reported in insects, lobsters and moles (Martin, 1965; Hangartner, 1967; Reeder and Ache, 1980;

Catania, 2013). However, the two strategies in the silkmoth are implemented as sequential behaviours (Fig. 1C, Fig. 5), and the spatiotemporal odour distribution would differentiate the use of each strategy. For example, at proximity to the odour source, osmotropotaxis would be dominant because silkmoths perform consecutive surges elicited by the repetitive odour stimuli, whereas the successive zigzagging and loop are dominant distant from the odour source or the centre of the plume because of the increasing intermittency of the odour. Therefore, with an increase in the frequency of odour reception, the repetitive surges facilitate both the osmotropotaxis and optomotor responses, which enable the moths to accurately orient towards the odour source according to the concentration gradients. However, the validity of the osmotropotaxis response in turbulent natural environments has not been demonstrated in silkmoths. We therefore suggest that the accuracy to track an odour gradient and the flexibility to track a wide range of odour distributions might also be adaptively balanced by odour contexts. The minimum concentration of the pheromone to trigger the surge (behavioural threshold) would be an essential factor. The behavioural threshold is not constant but is modulated by the serotonin concentration in the brain (Gatellier et al., 2004). Furthermore, a recent study indicated that projection neurons from the antennal lobe (the primary olfactory centre) encode the changes in the odorant concentration rather than the absolute concentration in the pulse trains of the pheromone, mimicking the odour distribution in nature (Fujiwara et al., 2014). Based on these studies, we speculate that the behavioural threshold would be ceaselessly modulated during odour tracking, which might adaptively alter the use of the two strategies and improve the efficiency of localization of the odour source.

Applicability of the insect-controlled robot for studies on the sensory-motor system

The insect-controlled robot fulfilled the requirements for the present study: a silkmoth tracks and localizes the odour source under the disturbed sensory-motor manipulations. Our robotic manipulation was non-invasive compared with previously used methods such as cutting, crossing or fixing antennae (Martin, 1965; Hangartner, 1967; Reeder and Ache, 1980; Kanzaki et al., 1992). Furthermore, we could put a tethered moth under the closed-loop condition where the moth can receive both external multiple sensory information and self-induced sensory feedback, which would be comparable to free-walking experiments. However, the difference in size between the robot and insects must be considered. In particular, the larger size of the wide tube gap compared with the antennal gap of silkmoths would facilitate the osmotropotaxis response. Although such an exaggerated experimental condition is certainly helpful for exploring the potential sensory-motor mechanisms in insects, we have no direct evidence that the freely walking silkmoths utilize the bilateral olfactory input in the natural setting, except for the simple observation of the behaviour in a wind tunnel (Takasaki et al., 2012). Odour reception is also affected by wing flapping (Loudon and Koehl, 2000); therefore, the direct measurement of the bilateral sensory input using instruments such as an electroantennogram will provide an answer to this question. We intend to carry out further investigations into how insects make use of sensory information in natural settings.

Acknowledgements

We thank Kiaran K. Lawson for providing assistance with image analysis and Shigeru Matsuyama for providing purified bombykol. We also thank the New Cosmos Electric Co., Ltd. for supplying us with the hot-wire semiconductor gas sensors, and Kenji Kawaguchi and Shigeru Nakao for their technical advice on the gas sensors.

Competing interests

The authors declare no competing or financial interests.

Author contributions

N.A. conceived, designed and performed the experiments, and analysed the data. N.A. and R.K. prepared the manuscript.

Funding

This work was supported by the Japan Society for the Promotion of Science KAKENHI [grant numbers 22700197, 24650090 to N.A.].

Supplementary information

Supplementary information available online at
http://jeb.biologists.org/lookup/suppl/doi:10.1242/jeb.124834/-/DC1

References

Ando, N., Emoto, S. and Kanzaki, R. (2013). Odour-tracking capability of a silkmoth driving a mobile robot with turning bias and time delay. *Bioinspir. Biomim.* **8**, 016008.

Baker, T. C. and Vogt, R. G. (1988). Measured behavioural latency in response to sex-pheromone loss in the large silk moth *Antheraea polyphemus*. *J. Exp. Biol.* **137**, 29-38.

Borst, A. and Heisenberg, M. (1982). Osmotropotaxis in *Drosophila melanogaster*. *J. Comp. Physiol. A* **147**, 479-484.

Budick, S. A. and Dickinson, M. H. (2006). Free-flight responses of *Drosophila melanogaster* to attractive odors. *J. Exp. Biol.* **209**, 3001-3017.

Catania, K. C. (2013). Stereo and serial sniffing guide navigation to an odour source in a mammal. *Nat. Commun.* **4**, 1441.

Chow, D. M. and Frye, M. A. (2008). Context-dependent olfactory enhancement of optomotor flight control in *Drosophila*. *J. Exp. Biol.* **211**, 2478-2485.

Crapse, T. B. and Sommer, M. A. (2008). Corollary discharge across the animal kingdom. *Nat. Rev. Neurosci.* **9**, 587-600.

Dickerson, B. H., Aldworth, Z. N. and Daniel, T. L. (2014). Control of moth flight posture is mediated by wing mechanosensory feedback. *J. Exp. Biol.* **217**, 2301-2308.

Duistermars, B. J., Chow, D. M. and Frye, M. A. (2009). Flies require bilateral sensory input to track odor gradients in flight. *Curr. Biol.* **19**, 1301-1307.

Emoto, S., Ando, N., Takahashi, H. and Kanzaki, R. (2007). Insect-controlled robot—evaluation of adaptation ability. *J. Robot. Mechatronics* **19**, 436-443.

Fujiwara, T., Kazawa, T., Sakurai, T., Fukushima, R., Uchino, K., Yamagata, T., Namiki, S., Haupt, S. S. and Kanzaki, R. (2014). Odorant concentration differentiator for intermittent olfactory signals. *J. Neurosci.* **34**, 16581-16593.

Gatellier, L., Nagao, T. and Kanzaki, R. (2004). Serotonin modifies the sensitivity of the male silkmoth to pheromone. *J. Exp. Biol.* **207**, 2487-2496.

Gaudry, Q., Nagel, K. I. and Wilson, R. I. (2012). Smelling on the fly: sensory cues and strategies for olfactory navigation in *Drosophila*. *Curr. Opin. Neurobiol.* **22**, 216-222.

Gaudry, Q., Hong, E. J., Kain, J., de Bivort, B. L. and Wilson, R. I. (2013). Asymmetric neurotransmitter release enables rapid odour lateralization in *Drosophila*. *Nature* **493**, 424-428.

Gomez-Marin, A., Duistermars, B. J., Frye, M. A. and Louis, M. (2010). Mechanisms of odor-tracking: multiple sensors for enhanced perception and behavior. *Front. Cell Neurosci.* **4**, 6.

Gomez-Marin, A., Stephens, G. J. and Louis, M. (2011). Active sampling and decision making in *Drosophila* chemotaxis. *Nat. Commun.* **2**, 441.

Hangartner, W. (1967). Spezifität und Inaktivierung des Spurpheromons von *Lasius fuliginosus* Latr. und Orientierung der Arbeiterinnen im Duftfeld. *Z. Vergl. Physiol.* **57**, 103-136.

Holm, S. (1979). A simple sequentially rejective multiple test procedure. *Scand. J. Stat.* **6**, 65-70.

Kaissling, K. E. (1997). Pheromone-controlled anemotaxis in moths. In *Orientation and Communication in Arthropods*, Vol. 84 (ed. M. Lehrer), pp. 343-374. Basel: Birkhäuser.

Kanzaki, R. (1998). Coordination of wing motion and walking suggests common control of zigzag motor program in a male silkworm moth. *J. Comp. Physiol. A Sens. Neural Behav. Physiol.* **182**, 267-276.

Kanzaki, R. (2007). How does a microbrain generate adaptive behavior? *Int. Congr. Ser.* **1301**, 7-14.

Kanzaki, R. and Mishima, T. (1996). Pheromone-triggered 'flipflopping' neural signals correlate with activities of neck motor neurons of a male moth, *Bombyx mori*. *Zool. Sci.* **13**, 79-87.

Kanzaki, R., Sugi, N. and Shibuya, T. (1992). Self-generated zigzag turning of *Bombyx mori* males during pheromone-mediated upwind walking. *Zool. Sci.* **9**, 515-527.

Kennedy, J. S. (1983). Zigzagging and casting as a programmed response to wind-borne odour: a review. *Physiol. Entomol.* **8**, 109-120.

Kennedy, J. S. and Marsh, D. (1974). Pheromone-regulated anemotaxis in flying moths. *Science* **184**, 999-1001.

Kramer, E. (1975). Orientation of the male silkmoth to the sex attractant bombykol. In *Olfaction and Taste*, Vol. 5 (ed. D. A. Denton and J. P. Coghlan), pp. 329-335. New York: Academic Press.
Kramer, E. (1997). A tentative intercausal nexus and its computer model on insect orientation in windborne pheromone plumes. In *Insect Pheromone Research* (ed. R. Cardé and A. Minks), pp. 232-247. USA: Springer.
Loudon, C. and Koehl, M. A. R. (2000). Sniffing by a silkworm moth: wing fanning enhances air penetration through and pheromone interception by antennae. *J. Exp. Biol.* **203**, 2977-2990.
Mafra-Neto, A. and Carde, R. T. (1994). Fine-scale structure of pheromone plumes modulates upwind orientation of flying moths. *Nature* **369**, 142-144.
Martin, H. (1965). Osmotropotaxis in the honey-bee. *Nature* **208**, 59-63.
Mishima, T. and Kanzaki, R. (1999). Physiological and morphological characterization of olfactory descending interneurons of the male silkworm moth, *Bombyx mori*. *J. Comp. Physiol. A Sens. Neural Behav. Physiol.* **184**, 143-160.
Murlis, J. and Jones, C. D. (1981). Fine-scale structure of odour plumes in relation to insect orientation to distant pheromone and other attractant sources. *Physiol. Entomol.* **6**, 71-86.
Namiki, S., Iwabuchi, S., Pansopha Kono, P. and Kanzaki, R. (2014). Information flow through neural circuits for pheromone orientation. *Nat. Commun.* **5**, 5919.
Olberg, R. M. (1983). Pheromone-triggered flip-flopping interneurons in the ventral nerve cord of the silkworm moth, *Bombyx mori*. *J. Comp. Physiol. A* **152**, 297-307.
Pansopha, P., Ando, N. and Kanzaki, R. (2014). Dynamic use of optic flow during pheromone tracking by the male silkmoth, *Bombyx mori*. *J. Exp. Biol.* **217**, 1811-1820.
Pinheiro, J., Bates, D., DebRoy, S., Sarkar, D. and **the R Development Core Team**. (2013). nlme: Linear and nonlinear mixed effects models. R package version 3.1-113. http://CRAN.R-project.org/package=nlme
R Development Core Team (2010). R: A language and environment for statistical computing. http://www.R-project.org.
Reeder, P. B. and Ache, B. W. (1980). Chemotaxis in the florida spiny lobster, *Panulirus argus*. *Anim. Behav.* **28**, 831-839.
Sane, S. P., Dieudonne, A., Willis, M. A. and Daniel, T. L. (2007). Antennal mechanosensors mediate flight control in moths. *Science* **315**, 863-866.
Sperry, R. W. (1950). Neural basis of the spontaneous optokinetic response produced by visual inversion. *J. Comp. Physiol. Psychol.* **43**, 482-489.
Takasaki, T., Namiki, S. and Kanzaki, R. (2012). Use of bilateral information to determine the walking direction during orientation to a pheromone source in the silkmoth *Bombyx mori*. *J. Comp. Physiol. A* **198**, 295-307.
Therneau, T. (2014). A package for survival analysis in S. R package version 2.37-37, http://CRAN.R-project.org/package=survival.
Tobin, T. R. (1981). Pheromone orientation: role of internal control mechanisms. *Science* **214**, 1147-1149.
Tobin, T. R. and Bell, W. J. (1986). Chemo-orientation of male *Trogoderma* variabile (Coleoptera, Dermestidae) in a simulated corridor of female sex pheromone. *J. Comp. Physiol. A* **158**, 729-739.
van Breugel, F. and Dickinson, M. H. (2014). Plume-tracking behavior of flying *Drosophila* emerges from a set of distinct sensory-motor reflexes. *Curr. Biol.* **24**, 274-286.
Vickers, N. J. (2000). Mechanisms of animal navigation in odor plumes. *Biol. Bull.* **198**, 203-212.
Vickers, N. J. (2006). Winging it: moth flight behavior and responses of olfactory neurons are shaped by pheromone plume dynamics. *Chem. Senses* **31**, 155-166.
Vickers, N. J. and Baker, T. C. (1994). Reiterative responses to single strands of odor promote sustained upwind flight and odor source location by moths. *Proc. Natl. Acad. Sci. USA* **91**, 5756-5760.
von Holst, E. and Mittelstaedt, H. (1950). Das Reafferenzprinzip - (Wechselwirkungen Zwischen Zentralnervensystem Und Peripherie). *Naturwissenschaften* **37**, 464-476.
Wada, S. and Kanzaki, R. (2005). Neural control mechanisms of the pheromone-triggered programmed behavior in male silkmoths revealed by double-labeling of descending interneurons and a motor neuron. *J. Comp. Neurol.* **484**, 168-182.
Webb, B. (2004). Neural mechanisms for prediction: do insects have forward models? *Trends Neurosci.* **27**, 278-282.
Willis, M. A. (2008). Chemical plume tracking behavior in animals and mobile robots. *Navigation* **55**, 127-135.
Willis, M. A. and Avondet, J. L. (2005). Odor-modulated orientation in walking male cockroaches *Periplaneta americana*, and the effects of odor plumes of different structure. *J. Exp. Biol.* **208**, 721-735.
Willis, M. A. and Baker, T. C. (1987). Comparison of manoeuvres used by walking versus flying *Grapholita molesta* males during pheromone-mediated upwind movement. *J. Insect Physiol.* **33**, 875-883.

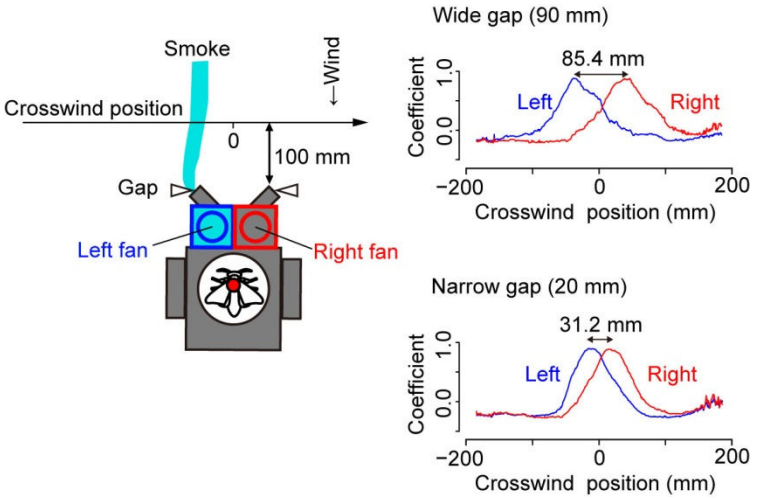

Fig. S1. Estimation of the odour sampling areas by different tube gaps.

The robot was placed in a wind tunnel with smoke (wind speed, 0.7 m s^{-1}), and the cross-correlations between the time-varying smoke density at arbitrary crosswind positions (x-axis, 100 mm ahead of the robot) and each fan [red (right) or blue (left) squares; lag, 0.3–0.4 s] were calculated by the tube positions with either wide (90 mm) or narrow (20 mm) gaps. The distance between the peaks of the cross-correlations on the right and left fans (wide, 85.4 mm; narrow, 31.2 mm) indicated that the tube gap effectively altered the odour sampling areas.

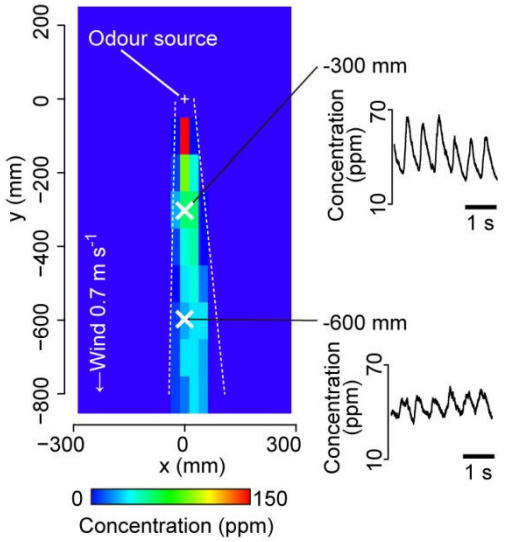

Fig. S2. Odour plume characterization and temporal property of the odour concentration in the robot using an ethanol plume.

The distribution of the mean ethanol concentration (indicated as colours) measured by a 25 mm × 50 mm grid is shown, in addition to the time course of the odour concentration in the canopy of the robot placed 300 mm and 600 mm downwind from the odour source (cross marks). An 80% of ethanol solution was used as odour (200 ms of ethanol puffing alternating with 300 ms pauses, stimulus frequency of 2 Hz) and the concentration was measured with a hot-wire semiconductor sensor (see Materials and methods). The broken lines indicate the estimated boundaries of the odour plume and the robot started at 600 mm downwind from the odour source in all the odour plume tracking tests.

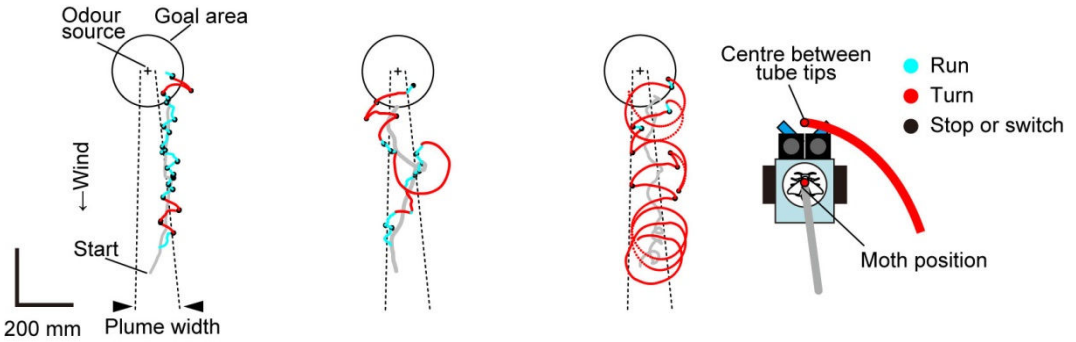

Fig. S3. Segmentation of behaviour.

We segmented each trajectory into two phases named run and turn. Three sample trajectories are displayed, ranging from smooth to complicated ones, in the non-covered control condition with a wide tube gap. In each trajectory, a grey line indicates the trajectory of the moth (the centre of rotation of the robot) and coloured lines indicate the trajectory of the centre between the two tube tips, to visualize turning more clearly. Cyan, red, and black colours indicate the run, turn, and stop or switch phases, respectively. The turn phase was used for the calculation of the mean turn angle (Figs. 2C and 3C), while both the turn and run phases were used for analysing the tendency to perform alternating short turns towards the odour source (Fig. 4C,D and supplementary material Fig. S8). The stop or switch phases were not used for analysis in this study.

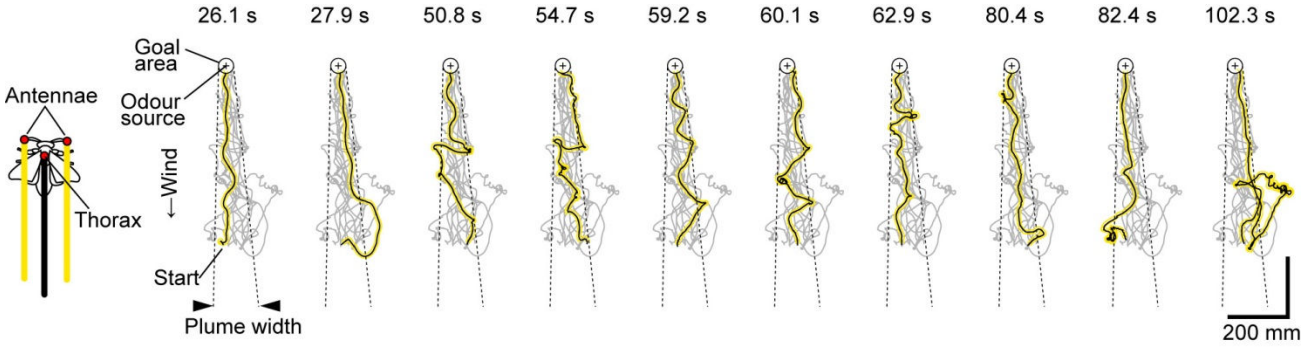

Fig. S4. Pheromone tracking behaviour of walking silkmoths.

Each of the ten trials is indicated by black (thorax) and yellow (antennal tips) lines, respectively. The other trajectories are indicated by grey lines. The time taken for localization is presented above each trajectory (median: 59.7 s). The experimental condition was the same as that in the robot except for a goal area (25 mm in radius) which was adjusted according to the size of the moths. Each moth was tested once and all ten moths succeeded in localizing the odour source.

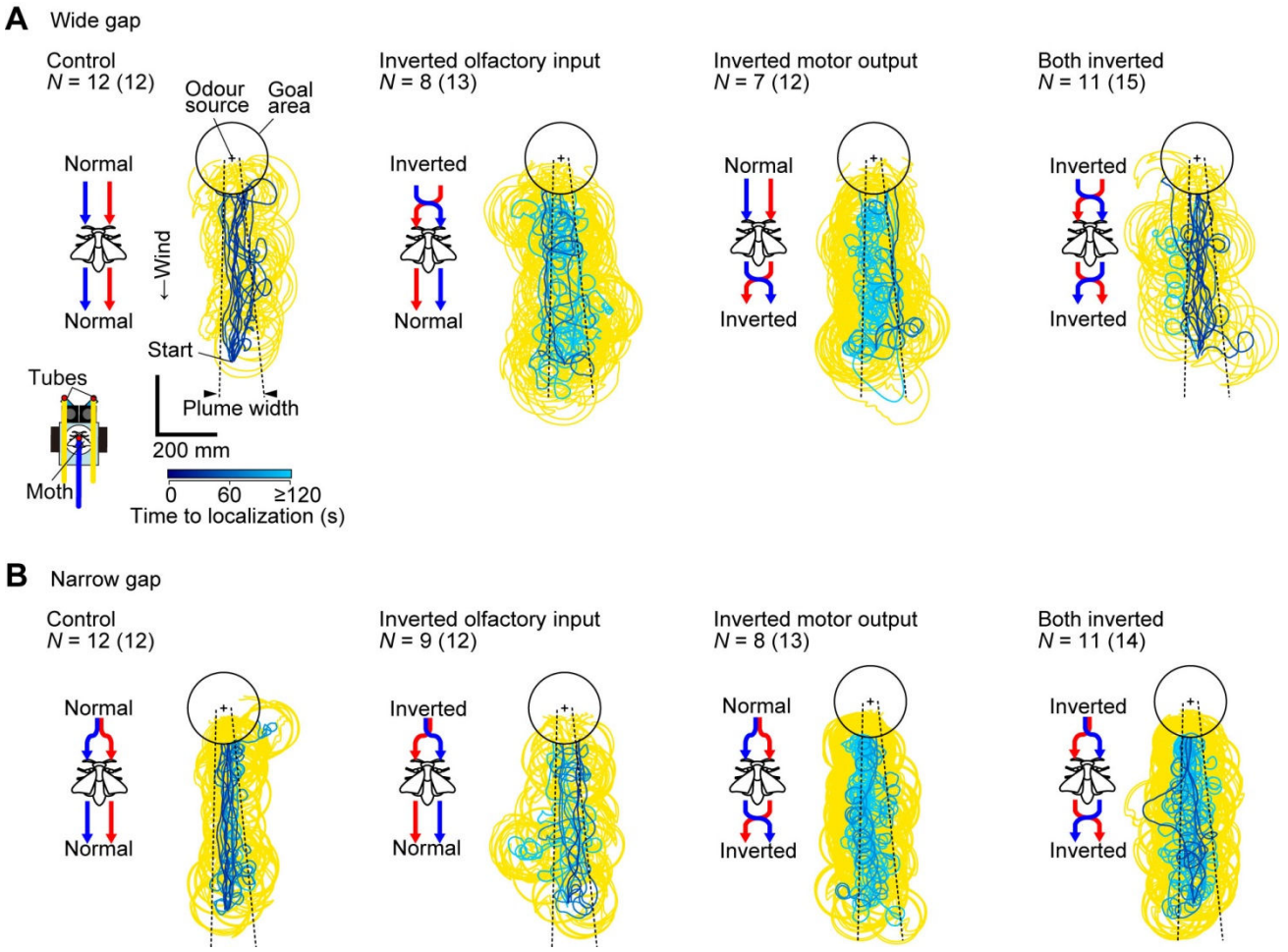

Fig. S5. Odour source localization of the robot in the different sensory-motor conditions.

(A, B) Trajectories of the robot with wide (A) and narrow (B) tube gaps. The trajectories from control (normal olfactory input and normal motor output), inverted olfactory input, inverted motor output and inverted olfactory input and inverted motor output are displayed. The trajectories with blue (brightness indicates time taken for localization in each trial) and yellow lines indicate the positions of the on-board moth (in the centre, between two wheels) and tips of the tubes, respectively. The number of successful trials is displayed, with the total number of trials in parentheses.

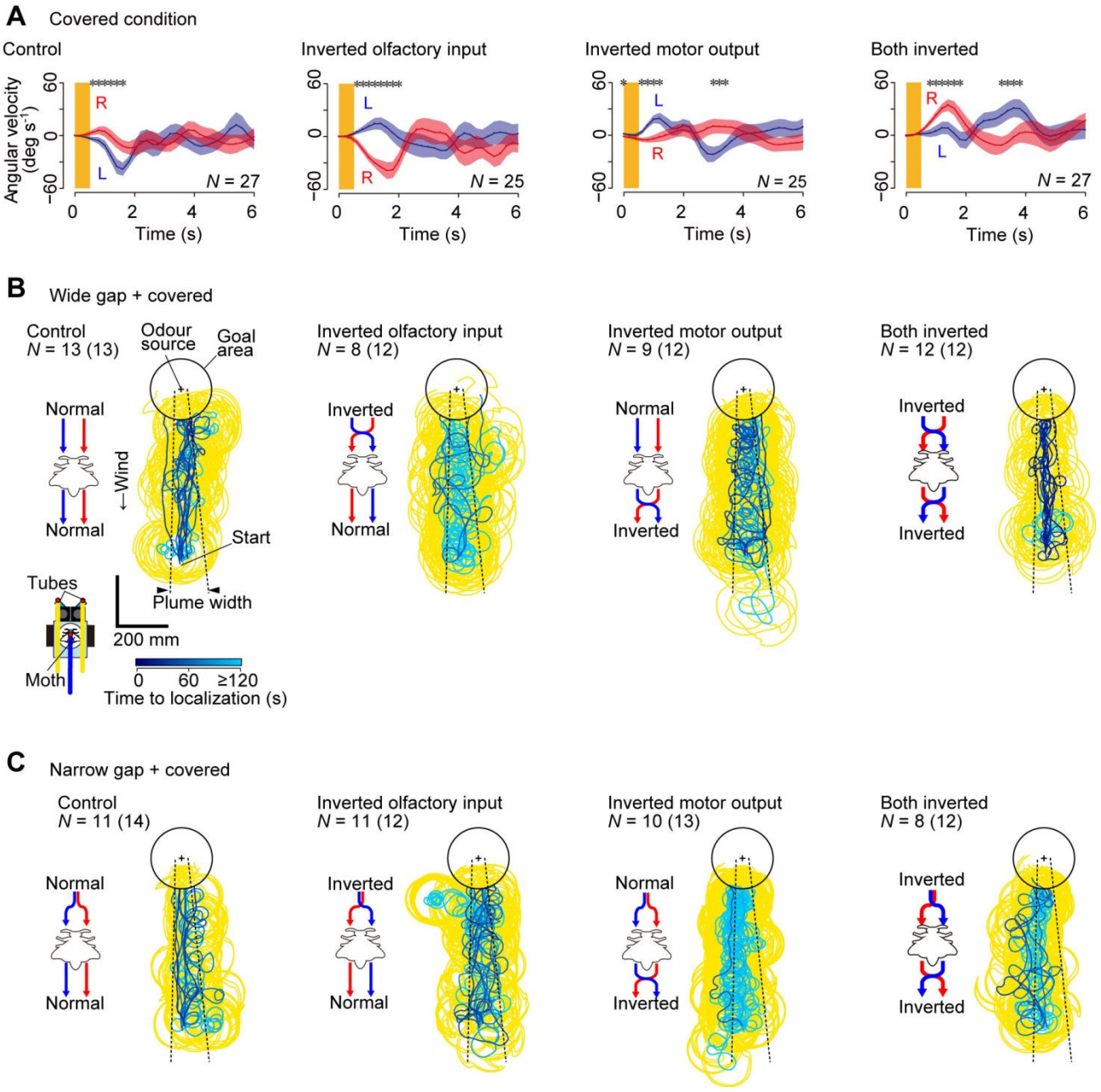

Fig. S6. Chemotactic turning responses and odour tracking trajectories of the covered robot.
(A) Time course of the angular velocity of the covered robot after a single puffed bombykol stimulus was applied to one of the air suction tubes. The red and blue lines indicate the mean angular velocity after the odour stimulus was applied to the right (R) and left side (L), respectively, averaged every 200 ms. The red and blue-shaded areas indicate the standard error. Positive and negative angular velocities indicate the clockwise and anticlockwise directions, respectively. The orange-shaded area indicates an odour stimulus of 2000 ng bombykol that was released over 500 ms. An asterisk indicates a significant difference in angular velocity between the stimulus sides at each 200-ms time bin (paired *t*-test, $*P<0.05$).

(B, C) Trajectories and mean resultant heading vectors of the robot with wide (B) and narrow (C) tube gaps under the covered condition. The trajectories from control (normal olfactory input and

normal motor output), inverted olfactory input, inverted motor output and inverted olfactory input, and inverted motor output are displayed. The trajectories with blue (brightness indicates time taken for localization in each trial) and yellow lines indicate the positions of the on-board moth (in the centre, between two wheels) and tips of the tubes, respectively. The number of successful trials is displayed, with the total number of trials in parentheses.

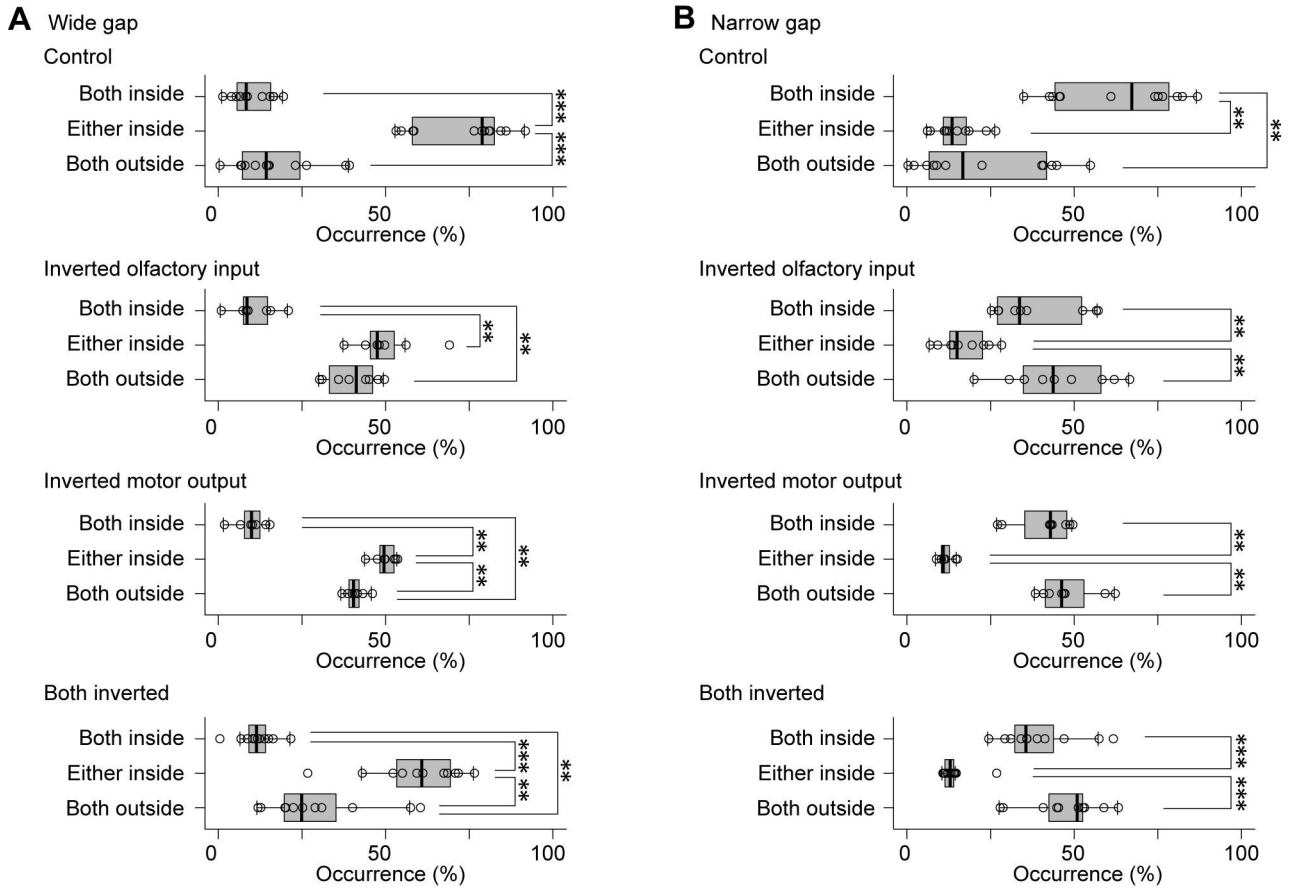

Fig. S7. Positions of the tube tips relative to the odour plume during behaviours.

The positions of the tube tips in trials with a large tube gap (A) and a narrow tube gap (B) were simply categorized into three situations: both tips were inside the plume (both inside), either tip was inside the plume (either inside), or both tips were outside the plume (both outside). The difference in the odour concentration between the right and left antennae of the moth is speculated to be large when either tip is inside the plume. In all the four conditions with the large gap, the occurrence of the either inside situation was significantly higher than that in the both inside situation, whereas the occurrence of the either inside situation was significantly lower than that in the both inside situation in conditions with the narrow tube gap. Comparisons between the tube situations were tested by the Steel-Dwass test (**P<0.01, ***P<0.001).

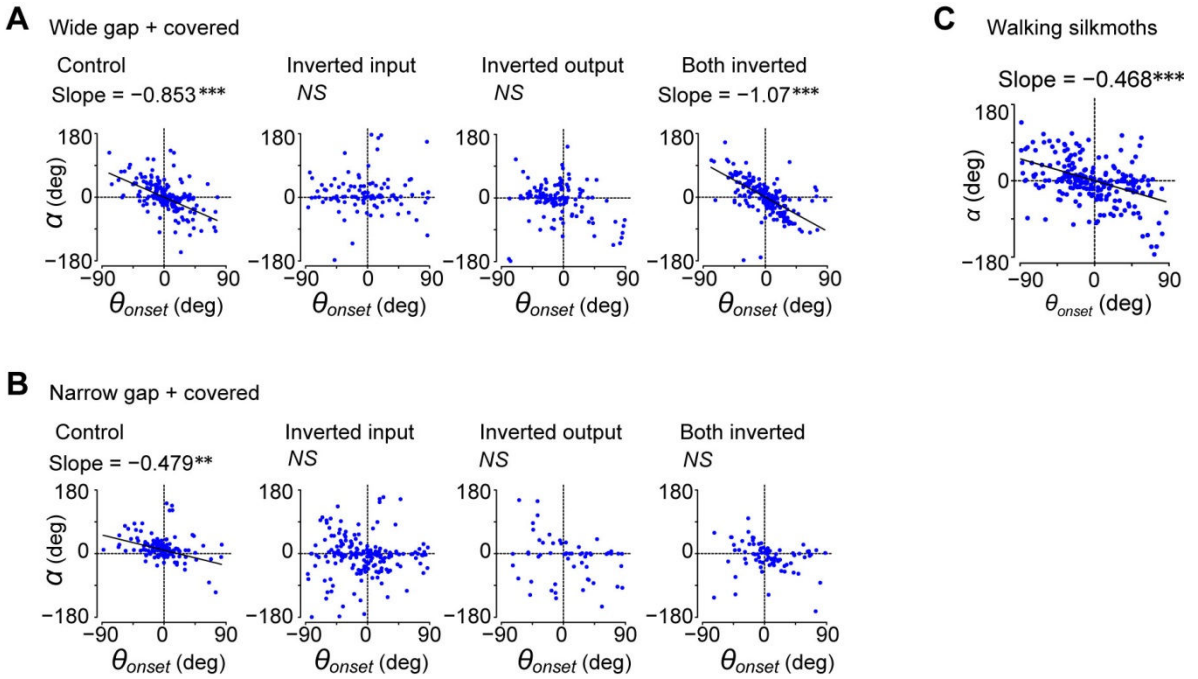

Fig. S8. Analyses of plume tracking behaviour of the covered robot and walking silkmoths.

(A, B) Relationship between the onset heading (θ_{onset}, $|\theta_{onset}| \leq 90°$) and turn angle ($\alpha$, $|\alpha| \leq 180°$) analysed by the linear mixed-effects models in covered conditions. Both wide gap (A) and narrow gap (B) conditions are shown. The variance between the trials was regarded as a random effect. Each of the blue points indicates a single behavioural segment (both run and turn phases were included). Each regression line indicates a fixed effect model in which a slope was statistically significant (not equal to 0; ***P*<0.01, ****P*<0.001; *NS*, non-significant, *P*>0.05).

(C) Relationship between the onset heading (θ_{onset}, $|\theta_{onset}| \leq 90°$) and turn angle ($\alpha$, $|\alpha| \leq 180°$) of the walking silkmoths during the pheromone plume tracking (the trajectories have been shown in supplementary material Fig. S4).

Table S1. The number of behavioural segments used for the linear mixed-effects model.

Experimental condition			Number of behavioural segments ($\lvert\alpha\rvert \leq 180°$, $\lvert\theta_{onset}\rvert \leq 90°$)			
Sensory-motor	Tube gap	Vision	Run	Turn	Total	*N*
Robot						
N-N	Wide		152 (98.1%)	51 (83.6%)	203 (94.0%)	12
I-N	Wide		114 (75.5%)	69 (46.3%)	183 (61.0%)	8
N-I	Wide		53 (76.8%)	29 (45.3%)	82 (61.7%)	7
I-I	Wide		87 (91.6%)	61 (69.3%)	148 (80.9%)	11
N-N	Narrow		153 (97.5%)	53 (60.2%)	206 (84.1%)	12
I-N	Narrow		115 (89.8%)	51 (53.7%)	166 (74.4%)	9
N-I	Narrow		42 (85.7%)	32 (40.5%)	74 (57.8%)	7 (8)
I-I	Narrow		73 (91.3%)	27 (38.0%)	100 (66.2%)	9 (11)
N-N	Wide	Covered	130 (96.3%)	72 (66.7%)	202 (83.1%)	13
I-N	Wide	Covered	67 (78.8%)	38 (38.8%)	105 (57.4%)	8
N-I	Wide	Covered	77 (78.6%)	47 (40.9%)	124 (58.2%)	9
I-I	Wide	Covered	97 (92.4%)	83 (80.6%)	180 (86.5%)	12
N-N	Narrow	Covered	105 (93.8%)	23 (46.9%)	128 (79.5%)	10 (11)
I-N	Narrow	Covered	110 (84.0%)	72 (53.7%)	182 (68.7%)	11
N-I	Narrow	Covered	28 (60.9%)	29 (30.2%)	57 (40.1%)	8 (10)
I-I	Narrow	Covered	60 (95.2%)	20 (34.5%)	80(66.1%)	7 (8)
Silkmoth			132 (88.6%)	93 (65.0%)	225 (77.1%)	10

The percentage in parentheses indicates the ratio of the behavioural segments used for the linear mixed-effects models (Figs. 4C,D and supplementary material Fig. S8) to the total number of behavioural segments. *N*, number of successful trials used for the linear mixed-effects models. Five trials from the four conditions were excluded from the analyses (the number in parentheses indicates the total number of the successful trials) because they did not contain more than two behavioural segments which corresponded to the criteria of the surge or short turn (see Materials and methods). For sensory-motor conditions, N–N, normal olfactory input and normal motor output; I–N, inverted olfactory input and normal motor output; N–I, normal olfactory input and inverted motor output; I–I, inverted olfactory input and inverted motor output.

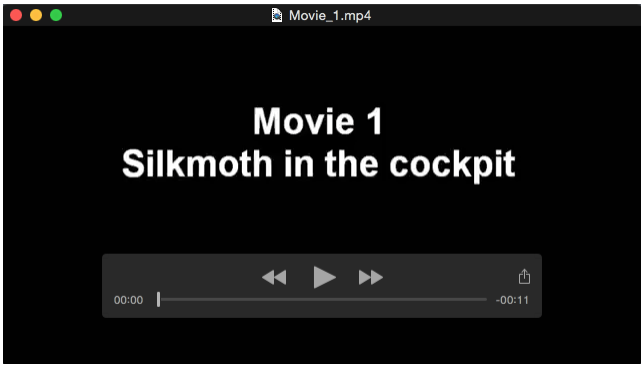

Movie 1. Silkmoth in the cockpit

Movie 2. Odour source localization of the robot with a wide tube gap
The trial with the median (or nearly the median) time taken for localization is displayed in each panel.

Movie 3. Odour source localization of the robot with a narrow tube gap
The trial with the median (or nearly the median) time taken for localization is displayed in each panel.

Movie 4. Odour source localization of the robot using a combination of surge and zigzagging
The movies corresponding to the trajectories in Fig. 4A and E–H are displayed.